Monodomain Simulations of Excitation and Recovery in Cardiac Blocks with Intramural Heterogeneity

Piero Colli Franzone[1], Luca F. Pavarino[2], and Bruno Taccardi[3]

[1] Dipartimento di Matematica, Universitá di Pavia and IMATI,
Istituto di Matematica Applicata e Tecnologie Informatiche,
Via Ferrata 1, 27100 Pavia, Italy
colli@imati.cnr.it
[2] Dipartimento di Matematica, Universitá di Milano,
Via Saldini 50, 20133 Milano, Italy
pavarino@mat.unimi.it
[3] Cardiovascular Research and Training Institute,
University of Utah, Salt Lake City, Utah
taccardi@cvrti.utah.edu

Abstract. Large scale simulations of an anisotropic and heterogeneous cardiac model in three dimensional myocardial blocks are presented. The Monodomain tissue representation used includes orthotropic anisotropy, intramural fiber rotation and homogeneous or heterogeneous intramural Luo-Rudy I membrane ionic models. Simulations of the entire QT interval for epicardial and endocardial pacing show that the effect of intramural heterogeneity on the dispersion of the action potential duration is mostly discernible along the epi- endocardial direction, while in the orthogonal directions the dispersion patterns have the same qualitative features of the homogeneous model.

1 Introduction

During a normal heartbeat, the ventricular transmembrane potential displays two main phases having different time and space scales: depolarization and repolarization. Repolarization exhibits a short rapid downstroke, a plateau and final, slower downstroke. While the excitation phase has been examined in considerable detail both experimentally and numerically much less is known concerning the recovery phase (see [8, 16, 7, 4]). Both phases are influenced by the fiber direction through which excitation is spreading and by the anisotropy of the intra and extracellular media. The study of these phases can be greatly enhanced by the use of computational models based on systems of differential equations. Previous studies considered simulations of the entire excitation and repolarization sequences mainly in 1D cables [10, 15, 17, 14] and 2D sheets, see e.g. [4]; only few simulation studies of a normal beat in 3D slabs are available in the literature, see e.g. [7, 9], even

A.F. Frangi et al. (Eds.): FIMH 2005, LNCS 3504, pp. 267–277, 2005.

if reentry dynamics have been largely studied. This is mainly due to the high computational costs involved in large scale simulations of a full cardiac cycle in three dimensions, which require adaptive and parallel numerical techniques. In [5], we implemented an efficient parallel simulator and performed several numerical experiments in 3D on parallel architectures with both the Monodomain and the Bidomain models. In [6], a detailed comparison between the excitation and the repolarization sequences elicited by a local stimulus showed that the Monodomain model is adequate for a qualitative investigation of the repolarization sequences and of the patterns displayed by the action potential duration (APD) distributions. Recently, the electrophysiological consequences of the intramural heterogeneity of the APD have generated considerable interest and some controversy. A subpopulation of cells (M cells) has been discovered, displaying a longer APD than epicardial and endocardial ventricular cell types, mainly in "in vitro" experiments, see e.g. [18]. On the other hand, high degrees of intramural heterogeneity have not been detected in "in vivo" studies of normal hearts, see e.g. [1], where it is noted that the intercellular coupling in cardiac tissue is a factor affecting APD modulation. However, controversy still exists over the extent to which heterogeneity in repolarization is expressed across the normal ventricular wall. In this work, we use our parallel simulator to investigate the influence of intramural heterogeneity of the intrinsic properties of the cellular membrane on the repolarization sequences and on the APD dispersion.

2 Mathematical Models

From a macroscopic point of view, the cardiac tissue is conceived as the superposition of two averaged continuous media, the intra and the extracellular medium, whose anisotropy is characterized by the conductivity tensors $D_i(\mathbf{x})$ and $D_e(\mathbf{x})$. These tensors are anisotropic related to the direction of the cardiac fibers that rotates counterclockwise (CCW) from epicardium to endocardium and to the laminar organization of the heart muscle (see [11]). Therefore, at any point $\mathbf{x}$, it is possible to identify a triplet of orthonormal principal axes $\mathbf{a}_l(\mathbf{x})$, $\mathbf{a}_t(\mathbf{x})$, $\mathbf{a}_n(\mathbf{x})$, with $\mathbf{a}_l(\mathbf{x})$ parallel to the local fiber direction, $\mathbf{a}_t(\mathbf{x})$ and $\mathbf{a}_n(\mathbf{x})$ tangent and orthogonal to the radial laminae respectively and both being transversal to the fiber axis. Denoting by $\sigma_l^{i,e}$, $\sigma_t^{i,e}$, $\sigma_n^{i,e}$ the conductivity coefficients measured along the corresponding directions, then the conductivity tensors $D_i(\mathbf{x})$ and $D_e(\mathbf{x})$ related to *orthotropic anisotropy* of the media are given by: $D_{i,e} = \sigma_l^{i,e}\ \mathbf{a}_l\mathbf{a}_l^T + \sigma_t^{i,e}\ \mathbf{a}_t\mathbf{a}_t^T + \sigma_n^{i,e}\ \mathbf{a}_n\mathbf{a}_n^T$.

The intra and extracellular electric potentials u_i, u_e in the Bidomain model are described by a reaction-diffusion system, coupled with a system of ODEs for ionic gating variables $w \in R^Q$ and for the ions concentration $c \in R^p$. Denoting by $v = u_i - u_e$ the transmembrane potential and by $I_{tot} = -D_i\nabla u_i - D_e\nabla u_e$ the total current flowing in the two media, then, for an insulated cardiac domain H, (v, u_e, I_{tot}, w, c) satisfy the system:

$$\begin{cases} c_m\partial_t v - \mathrm{div}(D_e D^{-1} D_i \nabla v) + I_{ion}(v,w) - \mathrm{div}(D_e D^{-1} I_{tot}) = 0, \\ \partial_t w - R(v,w) = 0, & w(\mathbf{x},0) = w_0(\mathbf{x}), \\ \partial_t c - S(v,w,c) = 0, & c(\mathbf{x},0) = c_0(\mathbf{x}), \\ \mathbf{n}^T D_m \nabla v = 0, & v(\mathbf{x},0) = v_0(\mathbf{x}), \\ I_{tot} = -D_i \nabla u_i - D_e \nabla u_e, \\ -\mathrm{div}(D\nabla u_e) = \mathrm{div}(D_i \nabla v), & -\mathbf{n}^T D \nabla u_e = \mathbf{n}^T D_i \nabla v, \end{cases}$$

where $\partial_t = \partial/\partial t$, $c_m = \chi * C_m$, $I_{ion} = \chi * i_{ion}$, with χ the ratio of membrane area per tissue volume, C_m the surface capacitance and i_{ion} the ionic current of the membrane per unit area. Disregarding applied currents, from the current conservation law, we have $\mathrm{div} I_{tot} = 0$. It is well known that, assuming equal anisotropy ratio of the two media, the Bidomain system reduces to the Monodomain model. If we disregard the source term $\mathrm{div}(D_e D^{-1} I_{tot})$, then a Monodomain model is derived as a Relaxed Bidomain system without assuming that the two tensors are proportional. Therefore, we obtain the anisotropic Monodomain model by solving first a single parabolic reaction-diffusion equation for the transmembrane potential v with the conductivity tensor given by $D_m = D_e D^{-1} D_i$ and coupled with the same gating and concentration system

$$\begin{cases} c_m\partial_t v - \mathrm{div}(D_e D^{-1} D_i \nabla v) + I_{ion}(v,w) = I_{app}, \\ \partial_t w - R(v,w) = 0, & w(\mathbf{x},0) = w_0(\mathbf{x}), \\ \partial_t c - S(v,w,c) = 0, & c(\mathbf{x},0) = c_0(\mathbf{x}), \\ \mathbf{n}^T D_m \nabla v = 0, & v(\mathbf{x},0) = v_0(\mathbf{x}), \end{cases}$$

and then solving an elliptic problem for the extracellular potential

$$-\mathrm{div}(D\nabla u_e) = \mathrm{div}(D_i \nabla v), \qquad -\mathbf{n}^T D \nabla u_e = \mathbf{n}^T D_i \nabla v.$$

We remark that the first equation is coupled with the system of ordinary differential equations in w, c and uncoupled from the elliptic equation in u_e; the system uniquely determines v, while the potential u_e is defined only up to an additive time-dependent constant related to the reference potential, chosen to be the average extracellular potential in the cardiac volume by imposing $\int_H u_e \, \mathrm{dx} = 0$.

3 Numerical Discretization

The cardiac volume H is discretized by a structured grid of hexahedral isoparametric Q_1 elements. A semidiscrete problem is obtained by applying a standard Galerkin procedure and choosing a finite element basis.

The time discretization is performed by a semi-implicit method using for the diffusion term the implicit Euler method, while the nonlinear reaction term I_{ion} is treated explicitly. The implicit treatment of the diffusion terms is essential in order to allow an adaptive change of the time step according to the stiffness of the various phases of the heartbeat. The ODE system for the gating variables is discretized by the semi-implicit Euler method and the explicit Euler method is applied for solving the ODE system for the ions concentration. We decouple the

full system by solving the gating and ions concentration system first (given the potential $\mathbf{v}^n$ at the previous time-step)

$$\mathbf{w}^{n+1} - \Delta t\ R(\mathbf{v}^n, \mathbf{w}^{n+1}) = \mathbf{w}^n, \qquad \mathbf{c}^{n+1} = \mathbf{c}^n + \Delta t\ S(\mathbf{v}^n, \mathbf{w}^{n+1}, \mathbf{c}^n)$$

and then solving for $\mathbf{v}^{n+1}$

$$\mathcal{A}_{\Delta t}\mathbf{v}^{n+1} = \mathrm{M}\Big[\frac{c_m}{\Delta t}\mathbf{v}^n - \mathrm{I}^h_{ion}(\mathbf{v}^n, \mathbf{w}^{n+1}, \mathbf{c}^{n+1}) + \mathrm{I}^{m,h}_{app}\Big],$$

where $\mathcal{A}_{\Delta t} = \frac{c_m}{\Delta t}\mathrm{M} + \mathrm{A}$, with A the stiffness matrix, M the mass matrix and $\mathrm{I}^h_{ion}, \mathrm{I}^{(m,e),h}_{app}$ the finite element interpolants of I_{ion} and $I^{m,e}_{app}$, respectively. We employed an adaptive time-stepping strategy based on controlling the transmembrane potential variation $\Delta v = max(\mathbf{v}^{n+1} - \mathbf{v}^n)$ at each time-step, see [12]. The linear system at each time step in the discrete problems is solved iteratively using the PETSc parallel library [2] and a preconditioned conjugate gradient solver with block Jacobi preconditioner and ILU(0) on each block. The parallel machines employed are an IBM SP RS/6000 Power4 with 512 processors Power 4 - 1300 MHz, (www.cineca.it), and a Cluster Linux with 72 Xeon 2.4 GHz processors. More details on the parallel solver can be found in [5].

4 Results

The cardiac domain considered is a cartesian slab of dimensions $5 \times 5 \times 1\ cm^3$ modeling a portion of the left ventricle. A structured grid of hexahedral isoparametric Q_1 elements of size $h = 0.1\ mm$ was used in all computations. In the numerical tests, we have used the following parameters: $\chi = 10^3\ cm^{-1}, C_m = 10^{-3}\ mF/cm^2$, $\{\sigma^e_l, \sigma^i_l, \sigma^e_t, \sigma^i_t\} = \{2,\ 3,\ 1.35,\ 0.315\}\ m\Omega^{-1}cm^{-1}$ and $\sigma^e_n = \sigma^e_t/2,\ \ \sigma^i_n = \sigma^i_t/10$. These conductivity coefficients of the orthotropic anisotropy have been calibrated so that the associated propagation velocities $(\theta_l, \theta_t, \theta_n)$ of ideal plane wavefronts can be conservatively estimated as (60, 25, 10) $cm\ sec^{-1}$, respectively. These estimates are in accordance with the histological findings of [11]) supporting the idea that the cardiac tissue anisotropy could be orthotropic. The fibers rotate intramurally linearly, proceeding counterclockwise (CCW) from epicardium (-45^o) to endocardium (75^o), for a total amount of 120^o. In this paper, we consider the phase I Luo-Rudy (LR1) model (see [12]), since it is one of the complex gating systems mostly used in recents 3D simulations. The initial conditions are at the rest and we apply an appropriate stimulus on a small area at the center of the slab (3 or 5 mesh points in each direction). Other than potentials and gating variables, at each time-step, we compute also the activation (ACTI) and the repolarization (REPO) times, defined as the times when the action potential (AP) crosses -60 mV during the upstroke and the downstroke, respectively; hence, the APD is defined as the difference APD = REPO - ACTI. . When homogeneous intrinsic properties of the cellular membrane are assumed, the slow inward current in the LR1 model is reduced by a factor 2/3, yielding an APD of about 266 msec. We also consider simulations with intramural

heterogeneity of the cellular membrane. In order to reproduce qualitatively the APD transmural behaviour measured in wedge preparations, see [18], Fig. 4 and [13] Fig. 5, we performed 1D simulations using a suitable subdivision of the wall thickness with different membrane properties. More precisely, we subdivided the slab into four layers of thickness (0.1, 0.1,0.7 0.1) cm, respectively, proceeding from the endo- to epicardium and by multiplying the slow inward current I_{si} of the LR1 model by (7.66, 8.66,7.86.6.66), corresponding to intrinsic APDs of (295,324,301,266), respectively. Hence we assume that sub-endocardial and mid-myocardial layers display a longer APD than the epi- and endo-cardial cells. The piecewise constant line in Fig. 1 (dashed) displays the intrinsic intramural APD distribution of the cells. We first consider a one-dimensional model having uniform conductivity equal to the intramural cross-fiber conductivity σ_t with homogeneous or heterogeneous intrinsic properties of the cellular membrane. In the homogeneous case (left panel of Fig. 1), the excitation and recovery fronts reach a quasi-stationary propagation, apart from the acceleration during the starting phase of the propagation and also during the subsequent collision with the endocardium. The total times for activation and recovery are about 39 and 32 msec, respectively, and the APD dispersion amounting to about 7 msec, mostly concentrated around the stimulus and collision sites. Notice that repolarization moves slightly faster than activation in the homogeneous model.

In the heterogeneous case (central panel of Fig. 1), the activation time results practically unchanged, while we have a higher repolarization time of about 54 msec. The APD dispersion, amounting to 21 msec, is three times larger than the homogeneous case. Due to current conduction, the intrinsic APD differences between the four cell layers are strongly smoothed and reduced. We have also applied an endocardial stimulus to the heterogeneous 1D model (right panel of Fig. 1). The sequence of excitation results the same as the one elicited by the epicardial stimulus, while the repolarization process is completed in 19 msec and the APD dispersion amounts to 28 msec. Therefore, an endocardial stimulus in the heterogeneous case brings about a significant shortening of the recovery sequence and a higher APD dispersion than an epicardial stimulus. In other words, epicardial stimulation increases the dispersion of the recovery time. We remark that these simulations are limited to an action potential elicited by a single stimulus, a condition that emphasizes the APD dispersion, since it is well known that a periodic stimulation, at an increasing rate, results in shortening of APD with a reduced dispersion.

We consider now 3D simulations of the excitation and repolarization processes elicited by an epicardial central stimulation in an orthotropic slab, homogeneous in Fig. 2, heterogeneous in Fig. 3. In both cases, we show the spread of excitation (ACTI), the sequence of recovery (REPO) and the APD on the whole slab (bottom) and on 5 plane sections parallel to the epicardial face, located at z = 0 (endo), 0.25, 5, 0.75, 1 (epi) cm, respectively. We now briefly describe some common features of the homogeneous and heterogeneous models. The spread of excitation and recovery exhibit an acceleration in the direction across fibers and dimple-like inflections appear in the isochrone profiles, due to

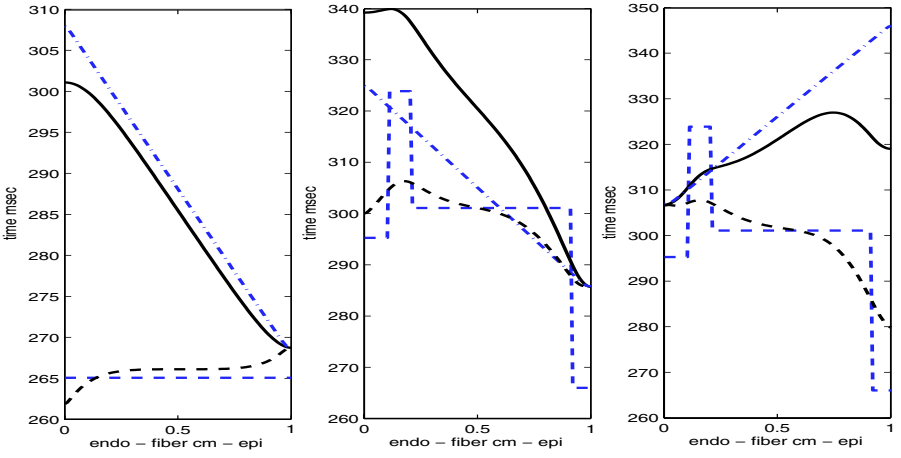

Fig. 1. Simulations along a fiber with conductivity coefficient σ_t of the intramural slab thickness. Activation, repolarization times and APD are displayed by dashed-dotted, continuous and dashed lines, respectively. Activation time has been shifted by the value of the repolarization time at the stimulus site. The piecewise constant line indicate the intrinsic APD of the cell layers. Left and Central Panels are related to an epicardial stimulation assuming homogeneous and heterogeneous intrinsic properties of the cellular membrane, respectively; the Rigth Panel refer to an endocardial stimulation for the heterogeneous case

the faster propagation of the fronts in deeper layers where the fiber direction rotates CCW relatively to the upper planes. The recovery isochrones on the epi, intramural and endocardial planes exhibit a somewhat smoother shape and slightly faster propagation compared with the excitation sequence. In particular, epicardial repolarization propagates across fibers faster than the excitation sequence, yielding a progressively APD shortening across fibers, as shown by Figs. 2,3. The APD patterns in both models are characterized by the following features: **i**) The APD distributions on the epicardial and intramural planes, exhibit a maximum located at the epicardial stimulation site or at the intramural points firstly reached by the excitation front, respectively; the level lines, surrounding these maxima, are elongated along the local fiber direction and display dog-bone shaped profiles. This indicates that APD decreases more rapidly when moving away from the center of the face in the cross-fiber direction than along fibers. **ii**) On the intramural sections (from subepicardial to midwall ones), two finger-shape valleys of decreasing APD values occur. These narrow valleys of relative APD shortening are located in the regions where excitation isochrones exhibit a dimple-like inflections. **iii**) On the endocardial plane the APD distribution displays a saddle point at the endocardial breakthrough; the APD increases reaching a maximum when moving away from the breakthrough point in a direction parallel to the endocardial fibers of 75^o CW. On the other hand, on the transmural sections displayed in Fig. 4 we see considerable differences be-

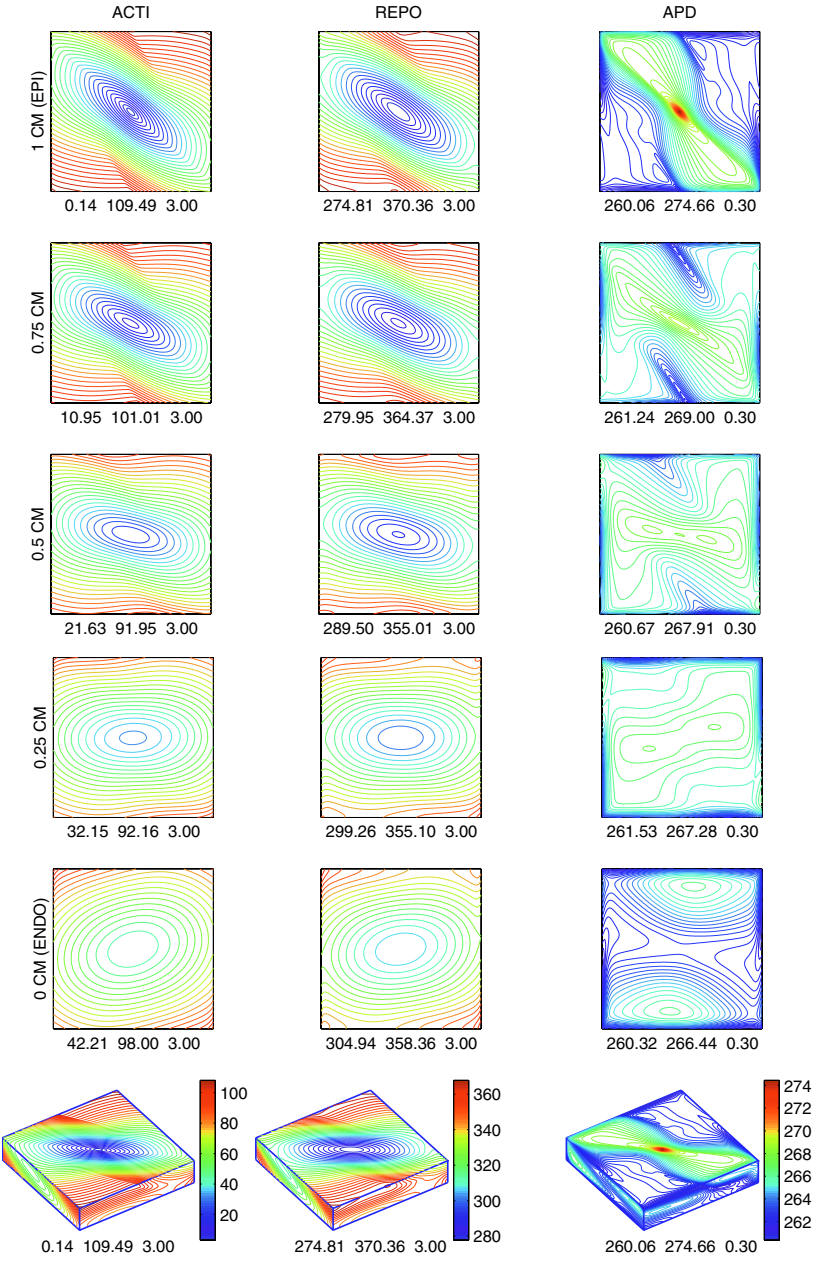

Fig. 2. Homogeneous tissue, orthotropic Monodomain slab $5 \times 5 \times 1 cm^3$. Isochrone lines of the depolarization time (first column ACTI), repolarization time (second column REPO) and action potential duration (third column APD) on 5 horizontal sections (z = 0, 0.25, 0.5, 0.75, 1 cm) and the whole slab; reported below each panel are the maximum, minimum and step in msec of the displayed map

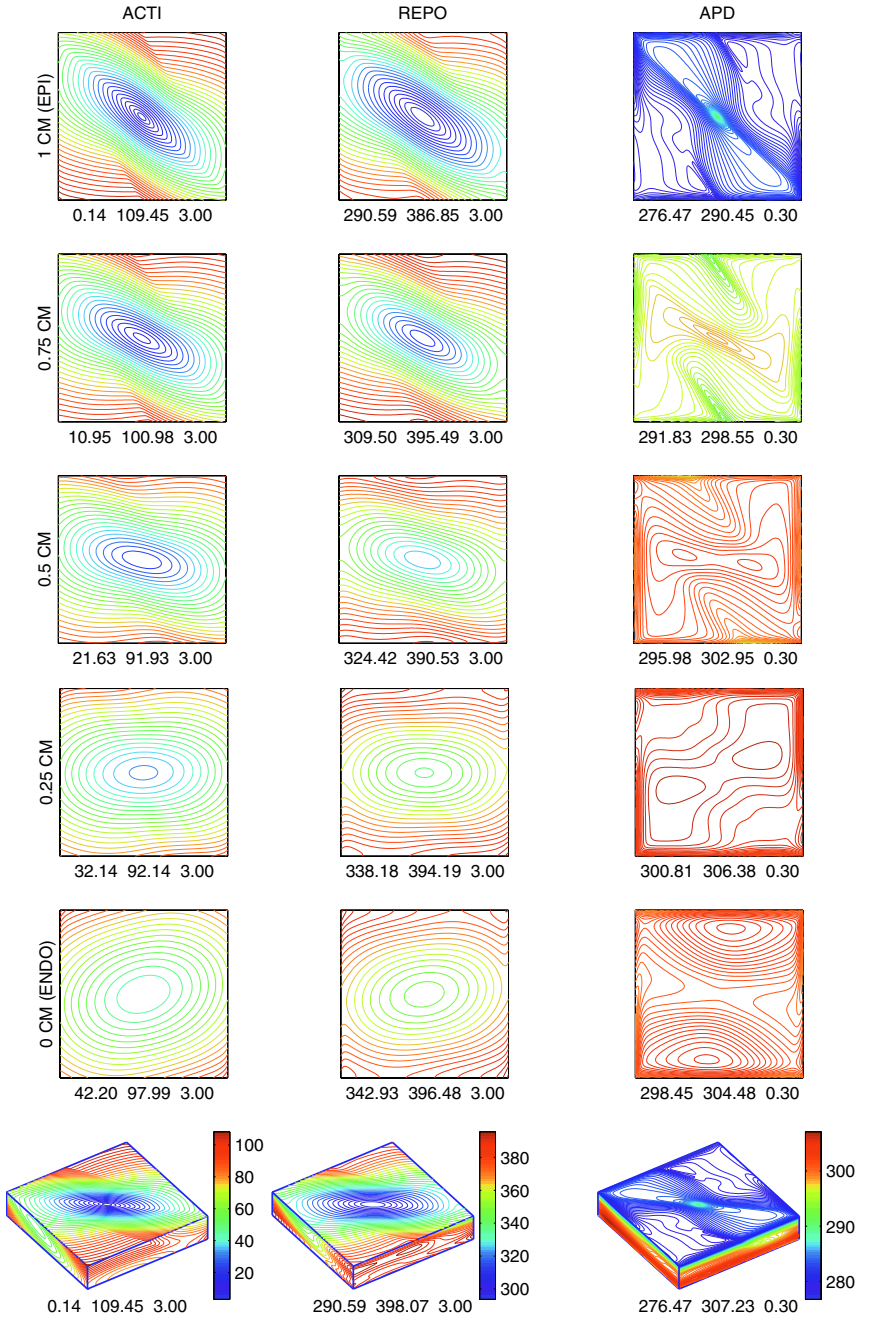

Fig. 3. Intramural heterogeneous tissue, orthotropic Monodomain slab $5 \times 5 \times 1 cm^3$. Same format as in Fig. 1

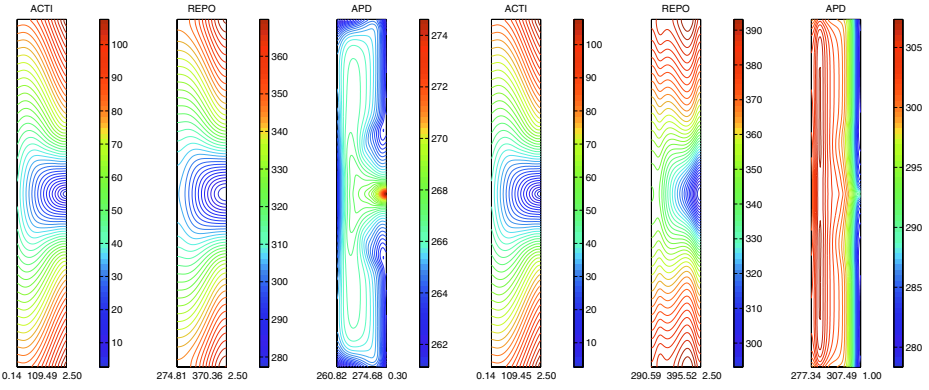

Fig. 4. Homogeneous tissue, orthotropic Monodomain slab $5 \times 5 \times 1 cm^3$. Isochrones of depolarization (first column ACTI), repolarization (second column REPO) times, action potential duration (third column APD) displayed on the transmural diagonal section perpendicular to the epicardial face and to the epicardial fiber direction. Left (right) three Panels refer to the homogeneous (heterogeneous) slab. Reported below each panel are the maximum, minimum and step in msec of the displayed map

tween the homogeneous and heterogeneous case. In both models the excitation isochrones on the transmural section show the presence of returning pathways, i.e. pathways that, starting from the epicardial stimulation site, proceed toward the endocardium but, about midway of the wall thickness, return toward the epicardial side. These pathways accelerate the propagation in epicardial areas where the excitation proceeds mainly across fibers. Return pathways of repolarization appear in the homogeneous slab whereas more complex recovery isochrone profiles are present in the heterogeneous model. In the heterogeneous model, the APD pattern shows parallel level lines stretched horizontally as opposed to the complex transmural APD pattern observed in the homogeneous slab. In planar sections parallel to the epicardial face, excitation and repolarization sequences and the spatial APD patterns elicited by endocardial pacing shared the same qualitative features as those described above for epicardial pacing in both the homogeneous and heterogeneous slab.

5 Conclusions

Our results show that, in spite of the homogeneous cellular membrane properties (i.e., all individual cells have the same intrinsic transmembrane action potential), the anisotropy of the media produces a spatial variation of the APD throughout the slab and the APD distribution exhibits anisotropic patterns strongly correlated with the excitation wave front motion and the front-boundary collisions.

The introduction of an intramural variation of the intrinsic cellular APD yields excitation and repolarization sequences and APD patterns which, on lay-

ers parallel to the epicardium, unexpectedly share the same main anisotropic spatial features encountered in the homogeneous slab, although recovery times and APDs exhibit a different range of values. The differences between the homogeneous and heterogeneous model remain confined transmurally for the repolarization and APD patterns while the excitation sequence does not change.

Anisotropic spatial variations of the APD along and across fibers were observed experimentally in 2D myocardial laminae in e.g. [8] and on the epicardium of dog hearts [3, 16]. We remark that simulation studies and experimental data have shown that excitation return pathways, proceedings toward the pacing level, have been observed for pacing sites located at any intramural level, from epi- to endo-cardium. Our simulated results show that clear repolarization return pathways are expected for the homogeneous slab.

In experimental studies in exposed and isolated dog hearts, the observed transmural dispersion of APD in the left ventricular wall is 30 msec at most, see e.g. [1]. Our unpublished experimental results confirm these findings, since during ventricular pacing with cycle length of 350 or 400 msec we observed 15-20 msec APD dispersion. In these preparations, the repolarization sequence was qualitatively similar to the activation sequence. When the pacing site was epicardial, both the excitation and the the repolarization "wave front" returned toward the epicardium in a transmural plane perpendicular to the epicardial fiber direction. However, further studies are needed to determine whether these findings occur consistently in varying experimental conditions. In this study, we have considered simulated beats by a single stimulus, a condition that emphasizes the APD difference and dispersion. Thus, our results show that transmural heterogeneities of APD cannot be detected from the epicardial pattern of the APD distribution.

References

1. Anyukhovsky E.P. et al.: The controversial M cell *J. Cardiovasc Electrophysiol*, 10: 244–260, 1999.
2. Balay S. and et al.: *PETSc Users Manual*. ANL TR anl-95/11 - rev. 2.1.5, 2002. http://www.mcs.anl.gov/petsc.
3. Burgess, M.J.B.and et al.: Nonuniform epicardial activation and repolarization properties of in vivo canine pulmonary conus. *Circ. Res.* 62 (2): 233–246, 1988.
4. Cates A.W. and Pollard A.E.: A model study of intramural dispersion of action potential duration in the canine pulmonary conus. *Ann. Biomed. Eng.*, 26: 567–576, 1998.
5. Colli Franzone P. and Pavarino L.F.: A parallel solver for reaction-diffusion systems in computational electrocardiology. *Math. Mod. Meth. Appl. Sci. (M3AS), 14 (6): 883–911*, 2004.
6. Colli Franzone P., Pavarino L.F. and Taccardi B.: Simulating patterns of excitation, repolarization and action potential duration with cardiac Bidomain and Monodomain models. *Submitted* , 2004.
7. Efimov I.R. et al.: Activation and repolarization patterns are governed by different structural characteristics of ventricular myocardium. *J. Cardiovasc. Electrophysiol.*, 7: 512–530, 1996.

8. Gotoh M. et al.: Anisotropic repolarization in ventricular tissue. *Am. J. Physiol.*, 41: 107–113, 1987.
9. Henriquez C. S and Penland R. C.: Impact of transmural structural and ionic heterogeneity on paced beats in the ventricle: a modeling study. *100 Years of Electrocardiology*, Schalit M.J. et al., Editors, Einthoven Foundation, 2002.
10. Joyner R. W.: Modulation of repolarization by electrotonic interactions. *Japan. Heart J.* 27: 167–183, 1986.
11. LeGrice I. J. et al.: Laminar structure of the heart: a mathematical model. *Am. J. Physiol. (Heart Circ. Physiol.)*, 272 (41): H2466-H2476, 1997.
12. Luo C. and Rudy Y.: A model of the ventricular cardiac action potential: depolarization, repolarization, and their interaction. *Circ. Res.*, 68: 1501–1526, 1991.
13. Poelzing S. et al.: Heterogeneous connexin43 expression produces electrophysiological heterogeneities across ventricular wall. *Am J. Physiol (Heart Circ. Physiol)*, 286: H2001-H2009, 2004.
14. Seeman G. et al.: Quantitative reconstruction of cardiac electromechanics in human myocardium. *J. Cardiovasc. Electrophysiol.*, 14: S219-S228, 2003.
15. Steinhaus B. M.: Estimating cardiac transmembrane activation and recovery times from unipolar and bipolar extracellular electrograms: a simulation study. *Circ. Res.* 64 (3): 449-462, 1989.
16. Taccardi B. et al.: Epicardial recovery sequences and excitation recovery intervals during paced beats. *PACE*, 22 (4) part II: 8–33, 1999.
17. Viswanathan,P. C. et al.: Effects of I_{Kr} and I_{Ks} heterogeneity on action potential duration and its rate dependence. *Circulation*, 99: 2466–2474, 1999.
18. Yan et al.: Characteristics and distribution of M cells in arterially perfused canine left ventricular wedge preparations. *Circulation*, 98: 1921–1927, 1998.